High-Resolution Computed Tomography Is Useful for Early Diagnosis of Severe Acute Respiratory Syndrome–Associated Coronavirus Pneumonia in Patients with Normal Chest Radiographs

Joyce Yee-Hing Hui, FRCR, Timothy Yu-Wai Hon, FRCR, Michael Kwok-Wai Yang, MBBS, Danny Hing-Yan Cho, MBBS, Wing-Hang Luk, FRCR, Ronee Yun-Yee Chan, FRCR, Kin-Sang Chan, FRCP, Tony Kwok-Loon Loke, FRCR, and James Chi-Sang Chan, FRCR

Objective: We investigated the usefulness of high-resolution computed tomography (HRCT) in early detection of severe acute respiratory syndrome (SARS)-associated coronavirus pneumonia and analyzed HRCT findings associated with potentially more severe disease.

Methods: All patients with suspected SARS and normal chest radiographs on admission within the study period were subjected to HRCT examination. The clinical, radiologic, and laboratory data of patients who were confirmed to have SARS-associated coronavirus infection by a positive nasopharyngeal aspirate, stool or urine reverse transcription-polymerase chain reaction (RT-PCR) and/or serological testing were prospectively followed up and analyzed. Characteristics of patients admitted to the intensive care unit (ICU) and those that were not were compared.

Results: Among 47 suspected SARS patients with normal chest radiographs, 27 had SARS-associated coronavirus infection confirmed by RT-PCR and/or positive serological testing. Twenty-five of the 27 (93%) patients had HRCT changes compatible with atypical pneumonia, and all 25 patients developed SARS with progressive clinical deterioration. Ten (40%) had unifocal diseases, and 15 had multifocal diseases (60%). Ten (40%) patients had the diseases confined to 1 single lung in the first HRCT, and both lungs were involved at initial presentation in 15 (60%) patients. Concerning the overall extent of the disease at initial presentation, 3 (12%) patients had disease process in all lobes, and the disease was confined to 1 single lobe in 10 (40%) patients. The disease process was mainly peripheral in location (96%), and the lower lobes were more commonly involved (68% in the left lower lobe and 64% in the right lower lobe). Small parapneumonic effusions occurred in 1 (4%) patient. None of the patients with unifocal lesions or single-lung involvement were admitted to the ICU ($P < 0.05$) (in both comparisons). Subsequent follow-up of the 2 (7%) patients with normal HRCT on admission showed that they were having nonpneumonic SARS-associated coronavirus infection only and were eventually denotified from having SARS.

Conclusions: HRCT is useful for early diagnosis of SARS-associated coronavirus pneumonia in patients with normal chest radiographs. HRCT findings in these patients predict potentially severe disease.

Key Words: atypical pneumonia, coronavirus, high-resolution computed tomography, severe acute respiratory syndrome

(*J Comput Assist Tomogr* 2004;28:1–9)

An outbreak of atypical pneumonia leading to the severe acute respiratory syndrome (SARS) has recently occurred in our community. Evidence is accumulating that the disease is caused by a novel coronavirus.[1–5] The disease has high mortality, and the most efficacious treatment is still not established. A substantial number of health-care workers have been infected despite all sorts of preventive measures, and the disease is causing major concerns throughout the world. The public is recommended to seek medical advice if they develop a sudden high fever and 1 or more respiratory symptoms, especially those with known contact or history of travel to affected areas. We are now facing a huge group of patients who are highly alert to the condition and present early with nonspecific symptoms and signs that may suggest SARS. Chest radiographs are well-known to be insensitive in the detection of subtle abnormalities in the lungs, with blind areas on frontal view making up to 40% of the lung area and 25% of the lung volume.[6,7] All rapid diagnostic tests for SARS are still in their developmental phase and cannot be used to exclude SARS and are not useful for screening. Their sensitivities and specificities are yet to be established.[5]

From the Department of Diagnostic Radiology and Organ Imaging (Drs Hui, Hon, Yang, Cho, Luk, R. Y-Y. Chan, Loke, and J. C-S. Chan) and the Respiratory Division, Department of Medicine (Dr K-S. Chan), United Christian Hospital, Kwun Tong, Hong Kong

Reprints: Dr J. Y-H. Hui, Department of Diagnostic Radiology and Organ Imaging, United Christian Hospital, 130 Hip Wo Street, Kwun Tong, Hong Kong (e-mail: jhuiyh@yahoo.com.hk).

In view of the reliability and rapid availability of high-resolution computed tomography (HRCT) of the thorax in the detection of other pulmonary pathology,[8–11] it may play a role in the early diagnosis of SARS so that early infection control measures and contact tracing can be implemented. Previous studies with SARS were based on identification of the condition as defined by the World Health Organization (WHO) or Centers for Disease Control and Prevention (CDC) criteria.[12,13] Moreover, HRCT was performed relatively late in the course of the patient's illness. In this study, we investigated the usefulness of HRCT in early detection of patients with microbiologically confirmed SARS-associated coronavirus pneumonia. HRCT findings that are associated with potentially more severe diseases are also analyzed.

PATIENTS AND METHODS

All patients in this study were in-patients of the United Christian Hospital who were admitted from 26 March 2003 to 7 April 2003. Patients who were admitted with a fever of more than 38°C and a history of exposure to a patient with SARS or absence of response to empirical antimicrobial coverage for typical and atypical pneumonia would be included in our study. All patients with suspected SARS underwent frontal chest radiograph examination. Posteroanterior chest radiographs were performed whenever it was possible, and for those who were unable to stand, anteroposterior view would be taken. Patients with normal chest radiographs on admission were subjected to HRCT examination within 24 hours. Hospital records of patients who were confirmed to have SARS-associated coronavirus infection by a positive nasopharyngeal aspirate, stool or urine reverse transcription-polymerase chain reaction (RT-PCR) (specimens collected in the first week after admission) and/or serological testing (acute and convalescent serum samples were collected on day 1 and day 14 after admission)[4] were prospectively followed up. The clinical, radiologic, and laboratory data were analyzed. Prior approval to the study by the hospital research ethics committee was not required as the protocol was carried out as part of our standard investigation procedure.

All scanning was performed with a helical CT scanner (High Speed Advantage; GE Medical Systems, Milwaukee, WI). One-millimeter-thick transverse sections were obtained from the lung apices through the bases at 10-mm increments with the patients in the supine position during full inspiration. Images were reconstructed using a high-spatial frequency algorithm. The CT images were reviewed in cine formats at a computer workstation (CT Advantage Windows 3.1 Advantage; GE Medical Systems, Milwaukee, WI) by 2 thoracic radiologists (J.Y-H.H. and T.Y-W.H). Images were examined at both standard lung and soft tissue settings.

Increased lung opacification was defined as ground glass when there was a hazy increase in attenuation without obscuration of the pulmonary vasculature and as consolidation when there was obscuration of the pulmonary vessels. For lesions containing both ground glass and consolidative components, the predominant changes are counted as the pattern of reference. The pattern, distribution, and extent of pulmonary parenchymal abnormalities were recorded according to consensus opinion. The disease extent was evaluated both in terms of the number of lungs involved, lobes involved (the lingula was considered as a separate lobe), and the number of lesion(s) in each lobe. A lesion was regarded to be central in location if it occurred within the inner half of the lung field and peripheral in location if it involved only the peripheral one-half of the lung. The presence of any dilated airways within the abnormal lung was observed. Size of the largest diameter of ground-glass opacity and/or consolidation missed on the chest radiographs and their possible explanations were recorded. The presence of any thickened interlobular septum, thickening of intralobular interstitium, lymphadenopathy, pleural effusion, and cavitating lung lesion was also noted.

A comparison of characteristics was made between patients who were admitted to the intensive care unit (ICU) requiring oxygen therapy and ventilatory support and those who were not. The 2 patients with normal HRCT were excluded from statistical analysis. Analyses were performed using SPSS version 11 (SPSS, Chicago, IL). χ^2 test was used for categorical variables and Student t test for continuous variables. $P < 0.05$ was regarded as statistically significant. Multivariate analysis was not performed because of small sample size.

RESULTS

A total of 155 patients were admitted to the United Christian Hospital with suspected SARS from 26 March 2003 to 7 April 2003. HRCT of the thorax was performed in 47 (30%) patients with normal chest radiographs on admission. Among these 47 patients, 27 had diagnosis of SARS-associated coronavirus infection confirmed by RT-PCR and/or positive serological testing and were included in the analysis.

The clinical characteristics and laboratory findings of the 27 patients were tabulated and are summarized in Tables 1 and 2. The male to female ratio was 10:17. The median age was 41 years (range, 20–77 years). All were nonsmokers. The majority of our patients enjoyed good past health. Concerning the history of exposure, 19 (70%) patients were residents in an outbreak housing estate (Amoy Gardens) and 4 (15%) were health-care workers taking care of affected cases in our hospital (Table 2). Four (15%) patients had no known history of contact. All patients except 1 (96%) had fever. None of the 27 patients had shortness of breath or any positive physical sign on admission.

The HRCT findings of our patients were tabulated and are summarized in Tables 1 and 3. HRCT was performed at a median duration of 2 days (range, 0–6 days) from the onset of

TABLE 1. Clinical Characteristics and HRCT Findings in Patients With SARS-Associated Coronavirus Infection

Clinical Characteristics					HRCT Findings						
Patient No.	Sex/ Age	Underlying Disease	History of Exposure	ICU Care	Pattern	Lungs Affected	Air Bronchogram	Number of Lobes Affected	Zonal Predilection of Lesion(s) Central/Peripheral	Largest Diameter of GGO (mm)	Largest Diameter of Consolidation (mm)
1	M/39	Nil	Yes	No	UG	L	No	1	Central	23.9	NA
2	M/62	Nil	No	No	UG	L	Yes	1	Peripheral	96.2	NA
3	F/37	Nil	Yes	No	MGC	L + R	Yes	2	Peripheral	18.5	40.5
4	M/47	HT	Yes	Yes	MG	L + R	No	5	Peripheral	72.1	NA
5	F/53	HT	Yes	No	UG	L	No	1	Peripheral	65.3	NA
6	F/33	Nil	Yes	Yes	MGC	L + R	Yes	2	Peripheral	34.5	37.5
7	F/72	Nil	Yes	Yes	MGC	L + R	Yes	3	Peripheral	29.8	52.0
8	F/41	DM	Yes	No	MGC	L + R	Yes	4	Peripheral	47.9	52.9
9	F/23	Nil	Yes	No	UG	L	No	1	Peripheral	54.5	NA
10	F/25	Nil	Yes	No	UC	L	No	1	Peripheral	NA	22.9
11	F/37	Nil	Yes	No	MG	L + R	Yes	2	Peripheral	74.0	NA
12	F/23	Nil	Yes	No	MGC	L + R	Yes	2	Peripheral	13.0	63.8
13	F/47	Nil	Yes	Yes	MGC	L + R	No	6	Peripheral	15.1	28.0
14	F/26	Nil	Yes	No	UG	L	Yes	1	Peripheral	24.7	NA
15	M/24	Nil	Yes	No	UG	L	Yes	1	Peripheral	23.0	NA
16	F/46	Nil	No	No	N	NA	NA	NA	NA	NA	NA
17	M/77	HT	No	No	UC	R	No	1	Peripheral	NA	6.9
18	F/54	Nil	No	No	N	NA	NA	NA	NA	NA	NA
19	M/31	Nil	Yes	No	MG	L + R	Yes	5	Peripheral	63.3	NA
20	M/36	Nil	Yes	No	MG	L + R	Yes	6	Peripheral	35.7	NA
21	F/26	Nil	Yes	No	UC	L	Yes	1	Peripheral	NA	41.0
22	M/20	Nil	Yes	No	MGC	L + R	No	3	Peripheral	12.2	17.2
23	F/48	Nil	Yes	No	UG	L	Yes	1	Peripheral	47.2	NA
24	M/57	Nil	Yes	Yes	MG	L + R	No	6	Peripheral	53.3	NA
25	M/40	Nil	Yes	Yes	MG	L + R	Yes	5	Peripheral	67.5	NA
26	F/49	Nil	Yes	No	MG	L + R	No	2	Peripheral	41.1	NA
27	F/34	β-Thal-trait	Yes	No	MG	L + R	Yes	5	Peripheral	30.2	NA

HRCT, high-resolution computed tomography; SARS, severe acute respiratory syndrome; HT, hypertension; DM, diabetes mellitus; β-Thal-trait, β-Thalassemia trait; UG, unifocal ground-glass opacity; UC, unifocal consolidation; MG, multifocal ground-glass opacities; MGC, multifocal ground-glass opacity(ies) and consolidation(s); N, normal; L, left; R, right; L + R, left and right; NA, not available; GGO, ground-glass opacity.

symptom. Two (7%) patients had a completely normal HRCT on initial presentation. Ten (40%) had unifocal disease of which 7 (28%) were unifocal ground-glass opacity (Fig. 1) and 3 (12%) were unifocal consolidation (Figs. 2 and 3). Multifocal disease occurred in 15 (60%) patients. Eight (32%) of them had multifocal ground-glass opacities (Fig. 4) and 7 (28%) had multifocal ground-glass opacity(ies) and consolidation(s) (Fig. 5). None of the patients with a normal chest radiograph had multifocal consolidations on HRCT. Ten (40%) patients had their disease confined to 1 lung in the first HRCT, and both lungs were involved at initial presentation in 15 (60%) patients. The disease process was mainly peripheral in location (96%) whereas a predominant centrally locating disease occurred in only 1 patient (4%). The largest diameter of the ground-glass opacity and consolidation detected on HRCT in the current study were 96.2 mm and 63.8 mm, respectively. Small parapneumonic effusions occurred in 1 (4%) patient. None of our patients had cavitation or hilar lymphadenopathy at presentation.

Subsequent follow-up of the 2 patients with normal HRCT showed that they did not develop respiratory distress and were having normal chest radiographs or HRCT on follow-up. These patients were eventually denotified from having SARS and were regarded as having only nonpneumonic SARS-associated coronavirus infection. For those patients with abnormal HRCT, 6 (24%) out of 25 patients have been admitted to the ICU. The clinical, laboratory, and HRCT characteristics of the patients who were admitted to the ICU and

TABLE 2. Clinical Features, Physical Parameters, and Laboratory Findings on Admission in Patients With SARS-Associated Coronavirus Infection

History of Exposure	Number (%)
Positive	23 (85)
Live in Amoy Gardens	19 (70)
Staff caring for affected case	4 (15)
No history of contact	4 (15)

Presenting Symptoms	Number (%)
Fever	26 (96)
Chills	13 (48)
Rigors	3 (11)
Myalgia	14 (52)
Sore throat	8 (30)
Running nose	5 (19)
Malaise	9 (33)
Dizziness	3 (11)
Diarrhea	1 (4)
Cough	13 (48)
Sputum	4 (15)
Shortness of breath	0 (0)
Headache	6 (22)

Physical Parameters	Mean	SD	Range
Temp (°C)	38.4	0.78	37 to 40
Respiratory rate (per minute)	18.2	1.6	16 to 22
Sao_2 (%)	98	1.4	96 to 100

Clinical Chemistry	Mean (range)	Percentage of Abnormal (Ratio)	Normal Range
White cell count	6.5 (3.7 to 11.1)	—	4 to 11 × 10^9/L
Leukopenia	—	15 (4/27)	
Lymphocyte count	0.98 (0.3 to 4.1)	—	1 to 38 × 10^9/L
Lymphopenia (<1.0 × 10^9/L)	—	85 (23/27)	
Neutrophil count	4.9 (2.2 to 9.9)	—	1.8 to 7.5 × 10^9/L
Neutrophilia	—	19 (5/27)	
Platelet	179 (107 to 312)	—	150 to 400 × 10^9/L
Thrombocytopenia (<150 × 10^9/L)	—	22 (6/27)	
Lactate dehydrogenase	369 (261 to 523)	—	240 to 480 U/L
Increased lactate dehydrogenase	—	7 (2/27)	
Creatinine kinase	234 (36 to 1577)	—	26 to 140 U/L
Elevated creatinine kinase	—	33 (9/27)	
Alanine aminotransferase	26 (11 to 78)	—	<31 U/L
Elevated alanine aminotransferase	—	22 (6/27)	
C-reactive protein	45 (4 to 214)	—	<8
Elevated C-reactive protein	—	69 (11/16)	
Urea	4.9 (2.1 to 7.9)	—	3 to 8 mmol/L
Decreased urea	—	15 (4/27)	
Sodium	139 (126 to 145)	—	134 to 149 mmol/L
Hyponatremia	—	4 (1/27)	
Potassium	3.9 (3 to 4.9)	—	3.2 to 5.2 mmol/L
Hypokalemia	—	4 (1/27)	

SARS, severe acute respiratory syndrome.

TABLE 3. HRCT Features in Patients with SARS-Associated Coronavirus Pneumonia

HRCT Features	Number (%)
Pattern	
Unifocal disease	10 (40)
Unifocal ground-glass opacity	7 (28)
Unifocal consolidation	3 (12)
Multifocal disease	15 (60)
Multifocal ground-glass opacities	8 (32)
Multifocal consolidations	0 (0)
Multifocal ground-glass opacity(ies) and consolidation(s)	7 (28)
Lungs affected	
One lung	10 (40)
Left	9 (36)
Right	1 (4)
Both lungs	15 (60)
Lobe involved	
Left upper	11 (44)
Lingula	7 (28)
Left lower	17 (68)
Right upper	8 (32)
Right middle	9 (36)
Right lower	16 (64)
Number of lobes affected	
1	10 (40)
2	5 (20)
3	2 (8)
4	1 (4)
5	4 (16)
6	3 (12)
Air bonchogram	
Present	15 (60)
Absent	10 (40)
Zonal predilection	
Central	1 (4)
Peripheral	24 (96)
Interloblar septal thickening	11 (44)
Thickening of intralobular interstitium	10 (40)
Parapneumonic effusion	1 (4)
Cavitation	0 (0)
Hilar lymphadenopathy	0 (0)

HRCT, high-resolution computed tomography; SARS, severe acute respiratory syndrome.

those who were not were compared and are summarized in Table 4. None of the patients with unifocal lesions or single lung involvement were admitted to the ICU ($P < 0.05$) (in both comparisons). Those who were admitted to the ICU were shown to have significantly higher levels of serum lactate dehydrogenase ($P < 0.05$) and creatinine kinase ($P < 0.05$) on admission. Overall, 5 (20%) patients died.

DISCUSSION

HRCT is useful and sensitive for early detection and diagnosis of SARS-associated coronavirus pneumonia in patients with normal chest radiographs, and it complements chest radiographs and laboratory tests in diagnosis of patients with SARS-associated coronavirus pneumonia. Previous studies in patients with SARS were based on identification of the condition as defined by the WHO or CDC criteria.[12,13] In some studies, uniform causation of the disease by the same organism has not been proven. The presenting symptoms of SARS-associated coronavirus infection are often nonspecific with fever being the most consistent symptom occurring in 97% of the cases. Because patients in the current series were those who presented very early in their course of illness, none of them had any positive physical signs localized to the chest on initial clinical examination and on chest radiographs in contrast to those patients who were already in very critical clinical condi-

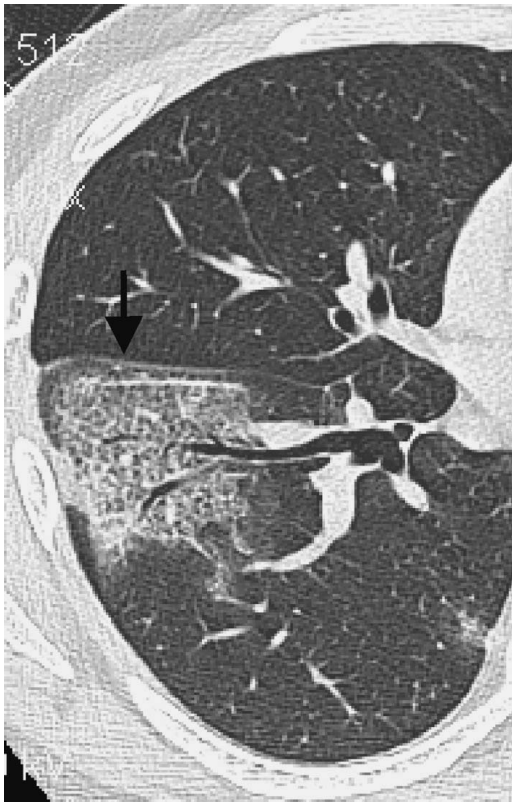

FIGURE 1. A 40-year-old man with SARS-associated coronavirus pneumonia. High-resolution computed tomography on day 3 from the onset of symptom shows a ground-glass opacification in the anterobasal segment of the right lower lobe, with prominent reticulation due to thickening of the interlobular septa and intralobular interstitium (arrow).

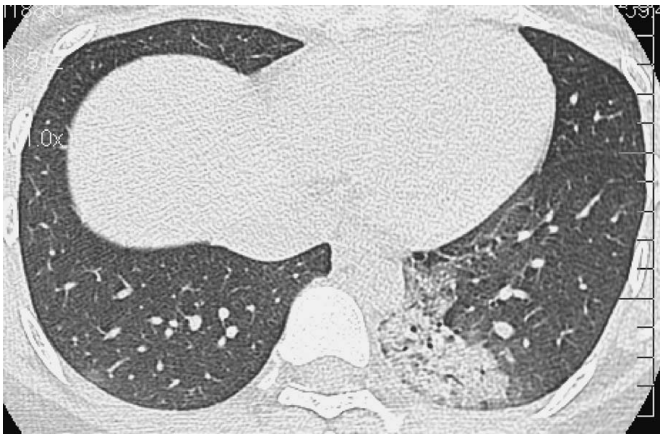

FIGURE 2. A 23-year-old woman with SARS-associated coronavirus pneumonia. High-resolution computed tomography on day 5 from the onset of symptom demonstrates a dense consolidation, with air bronchogram in the left lung base obscured by cardiac shadow.

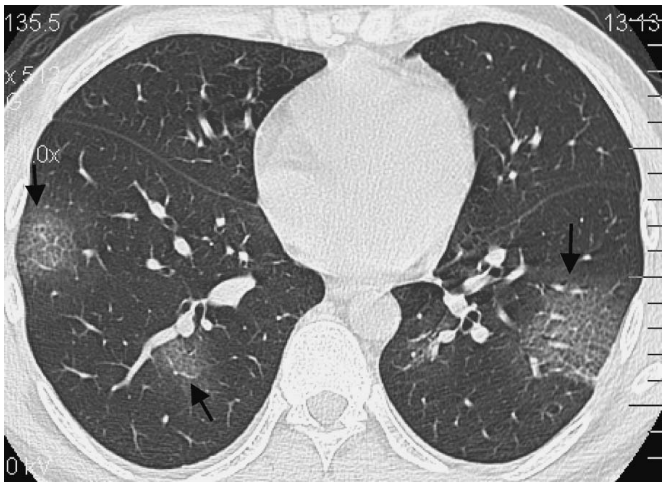

FIGURE 4. A 36-year-old man with SARS-associated coronavirus pneumonia. High-resolution computed tomography on day 3 from the onset of symptom shows multifocal ground-glass opacifications in the left and right lower lobes (arrows).

tion in other studies.[2,3] In these patients, HRCT changes are expected to precede chest radiograph abnormality. As SARS-associated coronavirus infection is a new disease entity, all the rapid diagnostic tests are still in their developmental phase; with their sensitivities and specificities unestablished, they cannot be used to exclude SARS. Although chest radiograph remains the most commonly used modality in the investigation and follow-up of patients with SARS coronavirus pneumonia, there are well-known regions in the frontal chest radiographs that are difficult to be assessed because of overlapping normal structures.[6] These known limitations and pitfalls of chest radiographs necessitate the use of HRCT, which has improved the detectability of many subtle and small lesions since its advent and has become an indispensable tool in the evaluation of suspected diffuse pulmonary disease during the past 15 years.[14] In the current study, 15 (60%) patients had their le-

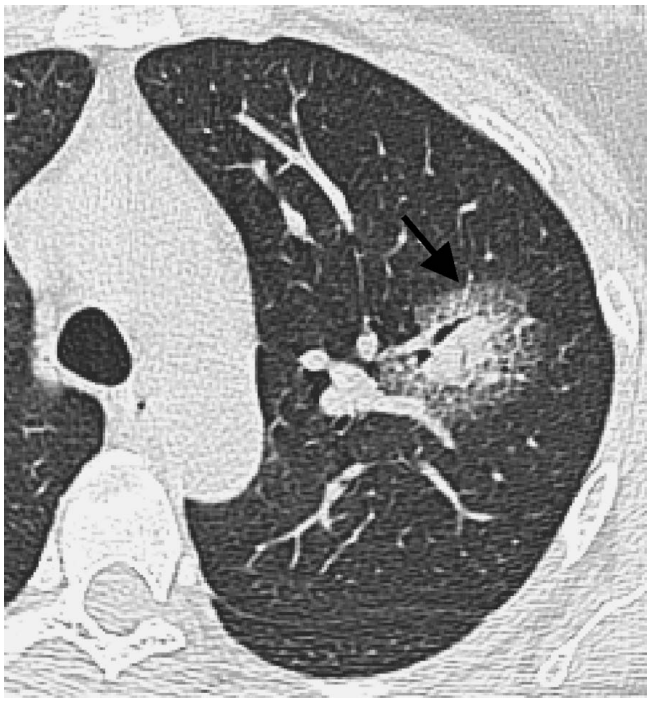

FIGURE 3. A 33-year-old woman with SARS-associated coronavirus pneumonia. High-resolution computed tomography on day 4 from the onset of symptom shows a centrally locating consolidation in the left upper lobe surrounded by a halo of ground-glass changes (arrow).

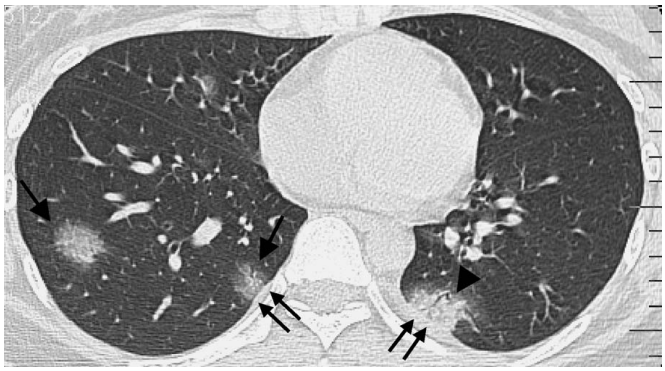

FIGURE 5. A 47-year-old woman with SARS-associated coronavirus pneumonia. High-resolution computed tomography on day 1 from the onset of symptom shows multifocal ground-glass opacities in the right middle and lower lobes (arrows). A consolidation (arrowhead) with air bronchogram is found in the left lower lobe. Small parapneumonic effusions (double arrows) are also seen.

TABLE 4. Risk Factors Associated with Severe Disease Requiring Ventilatory Support and Intensive Care

	Patients (%)		
	ICU Admission (n = 6)	**Non-ICU Admission (n = 19)**	***P* Value**
Age [year, mean (±SD)]	49.3 (±13.7)	37.4 (±15.0)	NS
Sex			
Male	3 (50)	7 (37)	NS
Female	3 (50)	12 (63)	
HRCT pattern			
Unifocal lesion	0 (0)	10 (53)	<0.05
Multifocal lesions	6 (100)	9 (47)	
Lung involved			
Single lung	0 (0)	10 (53)	<0.05
Both lungs	6 (100)	9 (47)	
Air bronchogram			
Present	3 (50)	12 (63)	NS
Absent	3 (50)	7 (37)	
Zonal predilection			
Central	0 (0)	1 (5)	NS
Peripheral	6 (100)	18 (95)	
White cell count [$\times 10^9$/L, mean (±SD)]	7.6 (±2.7)	5.9 (±1.9)	NS
Lymphocyte count [$\times 10^9$/L, mean (±SD)]	1.2 (±1.4)	0.8 (±0.4)	NS
Neutrophil count [$\times 10^9$/L, mean (±SD)	5.8 (±3.0)	4.7 (±1.8)	NS
Platelet count [$\times 10^9$/L, mean (±SD)]	148.5 (±35.7)	181.1 (±38.5)	NS
Lactate dehydrogenase [U/L, mean (±SD)]	453.4 (±69.9)	327.5 (±99.7)	<0.05
Creatinine kinase [U/L, mean (±SD)]	646.5 (±696.4)	109.3 (±56.6)	<0.05
Alanine aminotransferase [U/L, mean (±SD)]	30.3 (±7.7)	25.7 (±15.3)	NS
C-reactive protein [mg/L, mean (±SD)]	45.7 (±21.8)	68.5 (±74.0)	NS
Urea [mmol/L, mean (±SD)]	6.0 (±2.2)	4.6 (±1.53)	NS
Sodium [mmol/L, mean (±SD)]	136.3 (±5.7)	139.2 (±2.7)	NS
Potassium [mmol/L, mean (±SD)]	3.9 (±0.4)	3.8 (±0.4)	NS
Temperature [°C, mean (±SD)]	38.7 (±0.7)	38.4 (±0.8)	NS
Respiratory rate [per minute, mean (±SD)]	18.7 (±1.6)	18.0 (±1.5)	NS
So_{O_2} [%, mean (±SD)]	97.8 (±0.8)	98.3 (±1.5)	NS

ICU, intensive care unit; HRCT, high-resolution computed tomography.

sions missed on chest radiographs as they were merely subtle ground-glass opacities (Table 1). Four (16%), 2 (8%), 2 (8%), and 5 (20%) patients had their lesions in the chest radiographs obscured by the cardiac shadow, mediastinal structures, hila, and the diaphragm, respectively. The reason why there was an absence of multifocal consolidations on HRCT in the current series was because these lesions should readily be visible on chest radiographs. Although the HRCT features of patients with SARS coronavirus pneumonia are nonspecific and were indistinguishable from those associated with other causes of pneumonia, under the correct epidemiological setting, the use of HRCT adds confidence to the diagnosis of the condition. Infection control and contact tracing can then be started early.

HRCT helps to identify those patients who would eventually develop SARS. Out of these 27 patients with microbiologically confirmed SARS-associated coronavirus infection, 25 (93%) were found to have HRCT changes compatible with atypical pneumonia. Subsequent follow-up of these 25 patients shows that all of them developed SARS with progressive worsening of clinical symptoms. Interestingly, the 2 patients with normal HRCT did not have deterioration of their respiratory symptoms and did not develop pneumonic changes even after repeated chest radiographs and HRCT. They were subsequently confirmed not to have SARS. This implied that SARS-associated coronavirus is able to cause nonpneumonic infections that are clinically benign, and it may

be that only those patients who developed atypical pneumonia as identified by HRCT would develop SARS. Further studies are necessary to elucidate the spectrum and epidemiology of these nonpneumonic as well as subclinical coronavirus infections.

Although the HRCT changes in patients with SARS-associated coronavirus pneumonia were indistinguishable from the other causes of atypical pneumonia, there are several radiologic patterns that would support the diagnosis in patients with known contact and recent history of travel to infected areas. The pattern of radiologic progression of patients with SARS has recently been described.[15] The disease can be divided into 2 stages: the viral replicative phase and immunopathological damage. Furthermore, it was observed that during the early stage of the illness (viral replicative phase), lesions detected in the lungs appeared to be more focal and well defined in contrast to the irregular and ill-defined lesions in the late phase of the disease (immunopathological damage) which probably occurs as a result of systemic immune-mediated damage from the host to the lungs. In this study, multifocal disease was still a commoner presentation even in the early stage of the disease, and both lungs were involved in more than half of our patients; these despite the fact that individuals who had normal chest radiographs were expected to have fewer lesions detected on HRCT. This is because of the supreme ability of HRCT in the detection of small and subtle pulmonary abnormalities. Similar to other reported series,[13] the lower lobes were more commonly involved (68% in the left lower lobe and 64% in the right lower lobe), and the disease process was usually peripheral in location (96%). It was observed that consolidation up to 63.8 mm and ground-glass changes up to 96.2 mm in diameter could be missed by chest radiographs. This figure appeared to have slightly exaggerated the actual situation because consolidation and ground-glass changes are in fact a continuum. In our study, consolidation may have been encircled by a halo of ground-glass changes, but yet they were still classified as consolidation (Fig. 3). Small parapneumonic effusions occurred in 1 (4%) patient. None of our patients had cavitation or hilar lymphadenopathy at presentation.

In addition to helping in early diagnosis of SARS-associated coronavirus pneumonia, HRCT findings also predicted patients with subsequently more severe disease. In our study, a greater degree of pulmonary damage on initial HRCT as evident by the detection of abnormality in more than 1 lobe and bilateral lung involvement correlates well with severe complicated disease with oxygen desaturation, requiring ventilatory support in the ICU. None of the patients with unifocal lesions or single-lung involvement were admitted to the ICU ($P < 0.05$) (in both comparisons). Previous studies of pulmonary reovirus infection in athymic mice had shown that a lower plaque-forming value of 10^6 is associated with pathologic changes of bronchiolitis obliterans organizing pneumonia whereas a larger inoculum of 10^7 is associated with development of histologic characteristics of acute respiratory distress syndrome.[16] Moreover, similar to other studies,[3] those patients with more severe SARS were also found to have a higher serum lactate dehydrogenase and creatinine kinase level on admission. This means that the initial viral innocula in patients with SARS may be one of the factors affecting the subsequent disease severity. Early identification of these patients allows prompt treatment and close monitoring to be given to those who are at risk.

There are certain limitations to our study. First, this preliminary study was limited by the relatively small number of patients included. Second, there was also a lack of an age- and sex-matched control group of patients who had suspected SARS, but were subsequently confirmed not to have SARS-associated coronavirus infection. However, according to our preliminary experience, we have not seen a single patient with normal HRCT who developed SARS. Further studies are necessary to delineate the negative predictive value of HRCT in patients with suspected SARS.

CONCLUSIONS

Although the best logistics for diagnosis of SARS-associated coronavirus pneumonia depend on the availability of various microbiological tests and radiologic modalities in different centers, the current study had shown that HRCT is useful in early detection and diagnosis of SARS-associated coronavirus pneumonia before radiographic abnormalities were present. In the correct clinical and epidemiological settings, the presence of multifocal ground-glass opacity(ies) with or without consolidation(s) in the peripheral area of the lower lobes are highly suggestive of SARS-associated coronavirus pneumonia.

REFERENCES

1. Poutanen SM, Low DE, Henry B, et al. Identification of severe acute respiratory syndrome in Canada. *N Engl J Med*. 2003;348:1995–2005.
2. Tsang KW, Ho PL, Ooi GC, et al. A cluster of cases of severe acute respiratory syndrome in Hong Kong. *N Engl J Med*. 2003;348:1977–1985.
3. Lee N, Hui D, Wu A, et al. A major outbreak of severe acute respiratory syndrome in Hong Kong. *N Engl J Med*. 2003;348:1986–1994.
4. Peiris JSM, Lai ST, Poon LLM, et al. Coronavirus as a possible cause of severe acute respiratory syndrome. *Lancet*. 2003;361:1319–1325.
5. Ksiazek TG, Erdman D, Goldsmith C, et al. A novel coronavirus associated with severe acute respiratory syndrome. *N Engl J Med*. 2003;348:1953–1966.
6. Grainger RG, Allison DJ, Adam A, et al. *Diagnostic Radiology. A Textbook of Medical Imaging*. New York: Churchill Livingstone, 2001.
7. Meholic AJ, Ketai L, Lofgren RP. *Fundamentals of Chest Radiology*. Philadelphia: WB Saunders, 1996.
8. Hansell DM. High-resolution CT of diffuse lung disease: value and limitations. *Radiol Clin North Am*. 2001;39:1091–1113.
9. Muller NL, Staples CA, Miller RR. Bronchiolitis obliterans organizing pneumonia: CT features in 14 patients. *AJR Am J Roentgenol*. 1990;154:983–987.

10. McLoud TC. Occupational lung disease. *Radiol Clin North Am*. 1991;29: 931–941.
11. Webb WR. Radiology of obstructive pulmonary disease. *AJR Am J Roentgenol*. 1997;169:637–647.
12. Peiris JSM, Chu CM, Cheng VCC, et al. Clinical progression and viral load in a community outbreak of coronavirus-associated SARS pneumonia: a prospective study. *Lancet*. 2003;361:1767–1772.
13. Wong KT, Antonio GE, Hui DS, et al. Thin-section CT of severe acute respiratory syndrome: evaluation of 74 patients exposed to or with the disease. *Radiology*. (in press).
14. Webb WR, Muller NL, Naidich DP. High-resolution CT of the lung. Philadelphia: Lippincott Williams & Wilkins, 2001.
15. Hui JY, Cho DH, Yang MK, et al. Severe acute respiratory syndrome: spectrum of high-resolution CT findings and temporal progression of the disease. *AJR Am J Roentgenol*. (in press).
16. Majeski EI, Harley RA, Bellum SC, et al. Differential role for T cells in the development of fibrotic lesions associated with reovirus 1/L-induced bronchiolitis obliterans organizing pneumonia versus acute respiratory distress syndrome. *Am J Respir Cell Mol Biol*. 2003;28: 208–217.

